^{6}Li and ^{7}Li NMR line-shape and stimulated-echo studies of lithium ionic hopping in $LiPO_3$ glass

Sandra Faske, Hellmut Eckert, and Michael Vogel*
Institut für Physikalische Chemie, Westfälische Wilhelms-Universität Münster, Corrensstrasse 30, 48149 Münster, Germany
(Received 20 August 2007; revised manuscript received 10 December 2007; published 3 March 2008)

^{6}Li and ^{7}Li NMRs are used to investigate the lithium ion dynamics in $LiPO_3$ glass. In particular, ^{6}Li NMR stimulated-echo experiments are used to provide straightforward access to two-time correlation functions characterizing the lithium ionic hopping motion in the millisecond regime in a glassy ion conductor. Temperature-dependent measurements serve to separate the spin diffusion contribution and the dynamic contribution to the stimulated-echo decays. The ^{6}Li NMR correlation functions of $LiPO_3$ glass describing the lithium ionic motion show pronounced nonexponential decays, which can be well described by a stretched exponential function with a temperature-independent small stretching parameter $\beta=0.27$, indicating the complex nature of the lithium dynamics. The temperature dependence of the mean correlation times $\langle\tau\rangle$ resulting from these stimulated-echo experiments is described by an activation energy $E_a=0.66$ eV. The values of $\langle\tau\rangle$ are in good agreement with time constants from previous electrical and mechanical relaxation studies. At appropriate temperatures, the ^{6}Li and ^{7}Li NMR spectra are superpositions of a broad and a narrow spectral component, which result from slow and fast lithium ions, respectively, on the NMR time scale. A detailed analysis of the temperature dependence of these line shapes provides information about the distribution of correlation times.

DOI: 10.1103/PhysRevB.77.104301 PACS number(s): 66.30.Dn

I. INTRODUCTION

Lithium ion conducting glasses are technologically important for solid electrochemical devices such as batteries and chemical sensors.[1–4] Therefore, current fundamental research focuses on developing a microscopic understanding of ion transport in disordered solids. In such materials, elementary jumps of mobile ions between localized sites in a rigid matrix form the basis of the macroscopic transport. In general, the mechanism of ion hopping in glasses is complex, leading to strongly nonexponential ionic relaxation.[5] The origin of this nonexponentiality, which is a key feature of ion dynamics in solids, is still a subject of controversy.[6–12]

Being a fast ion conductor, glassy $LiPO_3$ serves as an ideal model compound for an examination of ion dynamics on a microscopic scale.[13–17] Results from electrical[13,16] and mechanical[16,17] relaxation studies indicate that the correlation function of the lithium ionic motion is well described by a Kohlrausch-Williams-Watts (KWW) function,[18,19]

$$\phi(t) = \exp\left[-\left(\frac{t}{\tau}\right)^{\beta}\right]. \quad (1)$$

Stretching parameters $\beta=0.33$ and $\beta=0.54$ were reported to characterize the nonexponentiality of the electrical[13,16] and mechanical[16,17] relaxations, respectively. On the basis of molecular dynamics (MD) simulations for $LiPO_3$ glass, it was demonstrated that both forward-backward jumps and a broad distribution of jump rates add to the complexity of the lithium ionic motion.[20,21]

In the present study, we exploit that modern solid-state NMR is a powerful tool to investigate the complex lithium ionic motion in solid electrolytes.[22] Analysis of NMR line shapes yields information about motions in the microsecond to millisecond regime since dynamics with correlation times τ of the order of the inverse linewidth lead to a narrowing of the static spectra. Motional narrowing has been observed in a wide variety of lithium-containing solid materials.[22] In addition, static NMR spectra can indicate the existence of a distribution of correlation times.[23,24] Besides the well-established spin-lattice relaxometry and line-shape analysis, recently developed multidimensional NMR techniques allow the study of ultraslow motions in the millisecond to second regime.[25] Two-dimensional NMR experiments in the frequency and in the time domain have yielded valuable information about time constants and the geometry of the motional processes in various supercooled liquids.[25–28] More recently, NMR multitime spectroscopy has been employed to characterize the ionic jumps in solid-state and polymer electrolytes.[22,29–44] Specifically, this technique was used to directly measure two-time correlation functions of lithium and silver ionic jump motions in glasses and crystals. Moreover, for silver ion conductors, three-time correlation functions indicated that, in large parts, the nonexponential ionic relaxation is due to a distribution of jump rates, i.e., dynamical heterogeneities, rather than to intrinsic nonexponentiality.[33,35,36,38] Very recently, ^{109}Ag four-time correlation experiments have shown that there is rapid rate exchange within these rate distributions and, hence, fast and slow silver ionic jumps alternate during the diffusion process.[36,39]

Lithium possesses two stable nuclear isotopes suitable for NMR studies, ^{6}Li and ^{7}Li, exhibiting spin quantum numbers $I=1$ and $3/2$, respectively. Because they differ greatly with respect to their magnetic dipole and electrical quadrupole moments, the NMR of these two isotopes can provide two different perspectives on the lithium dynamics in solid electrolytes. While analysis of line shapes and spin-lattice relaxation times provided valuable information about lithium ion conductors,[22,45–52] studies exploiting the potential of NMR multitime correlation functions are still rare. Thus far, ^{7}Li NMR two-time correlation functions have been measured to characterize lithium dynamics in a number of crystalline solid electrolytes,[29–31,37,40,41,43,44] and first studies of glasses have been performed as well.[22,37] However, in ^{7}Li NMR,

spin diffusion effects caused by strong dipolar couplings can complicate the interpretation of multitime correlation functions.[22] In addition, theoretical calculations have shown that the origin of the nonexponentiality can be determined by means of ^{7}Li three-time correlation spectroscopy.[53] At the present time, however, the pulse sequence has not been implemented because the spin-3/2 property necessitates the usage of rather complicated phase cycling schemes for appropriate coherence selection. A simpler solution is to turn to the other lithium isotope, ^{6}Li ($I=1$), for which the pulse sequences can be adopted from previous studies using ^{2}H as a probe nucleus.[25–28] In addition, the problems arising from dipolar couplings can be overcome for ^{6}Li, as will be demonstrated below. The potential disadvantage of using this isotope, namely, the low natural abundance in combination with long spin-lattice relaxation times, can be handled by isotopic enrichment.

In the present contribution, we use ^{6}Li and ^{7}Li NMRs to investigate the lithium jump dynamics in $LiPO_3$ glass. In particular, we will demonstrate that ^{6}Li NMR stimulated-echo spectroscopy is a powerful tool to investigate slow lithium ionic motion in solid electrolytes. Specifically, we will show that this technique provides access to single-particle correlation functions and, hence, yields well-defined information about ion dynamics on a microscopic level. While the present contribution represents the application of ^{6}Li NMR two-time correlation spectroscopy to a glassy ion conductor, Wilkening *et al.* have used it for characterizing lithium diffusion in a crystalline ion conductor.[54]

II. THEORY

A. Line-shape analysis

In studies of solid lithium ion conductors, an inherent NMR resonance frequency ω, mostly affected by the nuclear electric quadrupolar perturbation, can be ascribed to each ionic site. In glasses, different local environments result in distinguishable values of ω so that jumps between the ionic sites render the resonance frequency time dependent. The line shape of ^{6}Li nuclei in solids is dominated by the anisotropy of the nuclear electric quadrupolar interaction, which is expressed by[25]

$$\omega_Q = \frac{\delta_Q}{2}[3\cos^2\theta - 1 - \eta_Q \sin^2\theta\cos(2\phi)]. \tag{2}$$

Here, $\delta_Q = \frac{3e^2qQ}{4\hbar}$ for ^{6}Li ($I=1$) and $\delta_Q = \frac{e^2qQ}{2\hbar}$ for ^{7}Li ($I=3/2$). Furthermore, η_Q denotes the electric field gradient asymmetry parameter. The angles θ and ϕ specify the orientation of the electric field gradient tensor at the lithium site with respect to the external static magnetic flux density B_0. Typically, δ_Q is about $2\pi\times 100$ kHz for ^{7}Li, while it is a factor of about 50 smaller for ^{6}Li, which has the smallest quadrupole moment of all stable isotopes. However, the disorder in glasses leads to a range of electric field gradient values and, hence, to broad distributions of the δ_Q and η_Q values so that the spectra are structureless.[22]

In contrast to the situation in ^{6}Li NMR ($I=1$), the ^{7}Li NMR ($I=3/2$) spectra consist of two parts: a narrow line due to the $|1/2\rangle \leftrightarrow |-1/2\rangle$ central transition and a broad line due to the $|3/2\rangle \leftrightarrow |1/2\rangle$ and $|-1/2\rangle \leftrightarrow |-3/2\rangle$ "satellite transitions." The latter transitions are broadened due to the anisotropy of the quadrupolar interaction. Here, we analyze the width of the ^{7}Li central line, which is (to first order) not affected by quadrupolar coupling, but only by dipolar interactions. Since the dipolar coupling is a multiparticle interaction, this analysis does not provide access to single particle correlation functions. In ^{6}Li NMR, the two transitions, $|1\rangle \leftrightarrow |0\rangle$ and $|0\rangle \leftrightarrow |-1\rangle$, cannot be resolved due to the distribution of quadrupolar couplings. Therefore, only one single broad line is observed, which is Gaussian shaped. In ^{6}Li NMR, the quadrupolar interaction dominates, and thus single particle correlation functions are measurable; albeit, these are also influenced by multiparticle interactions owing to the effect of spin diffusion (see below).

The ^{6}Li and ^{7}Li resonance frequencies ω are modified by the stochastic process of lithium ionic jump motion. At low temperatures, when the correlation times are longer than the inverse width of the ^{6}Li and ^{7}Li NMR spectra, $\tau \gg \Delta\omega^{-1}$, the ionic motion does not affect the line shape and broad spectra are observed as a consequence of the different lithium ionic environments. Lithium ionic jumps on a time scale $\tau \approx \Delta\omega^{-1}$ lead to motional narrowing. In our case, $\Delta\omega$ is of the order of several hundreds of hertz, so that the NMR line shape is mainly sensitive to motion in the millisecond regime. Determination of the temperature T_{onset}, at which the motional narrowing sets in, allows one to obtain a rough estimate of the activation energy E_a of the lithium ionic jumps based on the formula of Waugh and Fedin,[55]

$$E_a(\text{eV}) \approx 1.617 \times 10^{-3}\, T_{onset}(\text{K}). \tag{3}$$

Using this equation, it is ignored that the value of the preexponential factor in the Arrhenius relation may differ considerably between different systems. At sufficiently high temperatures, the jump rates exceed the spectral dispersion, $\tau \ll \Delta\omega^{-1}$, and motionally averaged lithium NMR spectrum results. In order to relate the motional narrowing to the correlation time of the ionic jumps, it has also been common practice[22] to employ the equation first set forward by Bloembergen *et al.*,[56]

$$\tau_{LS} = \frac{1}{2\pi\alpha\Delta\nu}\tan\left(\frac{\pi}{2}\frac{\Delta\nu^2 - \Delta\nu_\infty^2}{\Delta\nu_0^2}\right). \tag{4}$$

Here, $\Delta\nu_0$ and $\Delta\nu_\infty$ are the linewidths of the static spectra in the limits of slow and fast motions, respectively. α is a fit parameter, normally chosen to be one. This formula was applied to the lithium ionic motion in amorphous $LiNbO_3$.[57]

We already mention that Eqs. (3) and (4) are of limited use, when the dynamical process is characterized by a broad distribution of correlation times $G(\log_{10}\tau)$. Then, line narrowing sets in at a temperature T_{onset} at which the fastest ions of the distribution exhibit $\tau \approx \Delta\omega^{-1}$. However, the mean correlation time, related to the center of gravity of the distribution, is much longer and, hence, Eq. (3) underestimates the activation energy, in particular, for wide distributions. Also, if a distribution $G(\log_{10}\tau)$ exists, the motional narrowing effects will be smeared out over a broad temperature range.

As a consequence, the temperature dependence of the correlation times determined from the linewidth according to Eq. (4) does no longer reflect the shift of the distribution $G(\log_{10}\tau)$. In the present contribution, we will demonstrate that, unlike line-shape analysis, ^{6}Li NMR stimulated-echo spectroscopy enables a measurement of meaningful correlation times of complex molecular dynamics.

Experimental[33,34] and computational[20,21] studies have shown that the ion dynamics in phosphate glasses are governed by very broad distributions of correlation times $G(\log_{10}\tau)$ so that fast ($\tau \ll \Delta\omega^{-1}$) and slow ($\tau \gg \Delta\omega^{-1}$) ions can be present at the same temperature. In this case, it is possible to describe the spectra as a superposition of sharp, motionally narrowed line and broad line, representing the situation in a rigid environment. Spectra of this kind have been called "two-phase" spectra.[23] The contribution from particles with $\tau \approx \Delta\omega^{-1}$ can be neglected for a broad distribution of correlation times usually found in glasses. Such two-phase spectra were observed in ^{109}Ag NMR studies on the silver ionic diffusion in silver phosphate[33,34] and borate[35] glasses. Then, the temperature-dependent normalized spectral intensity $S(\omega;T)$ can be written as[23]

$$S(\omega;T) = W(T)S_f(\omega) + [1 - W(T)]S_s(\omega). \tag{5}$$

Here, $S_f(\omega)$ and $S_s(\omega)$ are the normalized line shapes in the limits of fast and slow motions, respectively. The weighting factor $W(T)$ of the former spectral pattern ($0 \leq W \leq 1$) is related to the distribution of correlation times according to

$$W(T) = \int_{-\infty}^{\log_{10}\Delta\omega^{-1}} G(\log_{10}\tau;T)d\log_{10}\tau. \tag{6}$$

Based on the temperature dependence of the weighting factor, it is possible to get an estimate of the width of the distribution of correlation times $G(\log_{10}\tau)$. For this purpose, thermally activated jumps are assumed. In the first approach, we assume a logarithmic Gaussian distribution $G(\log_{10}\tau)$ with a temperature-independent width. Such a temperature independence is suggested by the time-temperature superposition principle found in frequency-dependent conductivity measurements.[58–60] In this case, the temperature-dependent shift of the center of the distribution $\log_{10}\tau_m(T)$ is related to the weighting factor by

$$W(T) = \frac{1}{2} + \frac{1}{2}\mathrm{erf}\left(\frac{\log_{10}\Delta\nu^{-1} - \log_{10}\tau_m(T)}{\sqrt{2}\sigma}\right), \tag{7}$$

where $\tau_m = \tau_0 \exp(E_a/T)$ and $\mathrm{erf}(x)$ is the error function.[24] Here, the width of the distribution of correlation times σ and the preexponential factor τ_0 are accessible, when fitting the experimental $W(T)$ to this function for a given value of E_a (see below). In the second approach, we assume that the static matrix in an ion conductor leads to a temperature-independent distribution of activation energies $g(E_a)$ so that a temperature-dependent width $G(\log_{10}\tau)$ results. Within this approach, $g(E_a)$ can be extracted from the line-shape analysis of NMR spectra measured as a function of temperature, according to[23]

$$\frac{dW(T)}{dT} = g(E_a)R\ln\left(\frac{\tau}{\tau_0}\right). \tag{8}$$

B. Two-time correlation functions

Multidimensional NMR techniques are sensitive to an exchange of frequencies during a experimentally defined mixing time.[25–28] Specifically, stimulated-echo experiments allow one to study dynamics with correlation times in the millisecond to second range. In the experiment, the NMR frequencies at two times are measured and correlated. For this purpose, the stimulated-echo pulse sequence is applied to manipulate the spin system. The pulses P_1-t_p-P_2-t_m-P_3-t_p divide the experimental time into two short evolution times, $t_p \ll \tau$ during which the spins are labeled according to their instantaneous NMR frequencies and longer mixing times $t_m \approx \tau$ during which dynamics may take place, leading to changes in the value of ω. Ions residing at the same site before and after t_m, i.e., ions showing the same ω during the two evolution periods, contribute to a stimulated echo at time t_p after the third pulse. When the height of this echo is measured for various t_m, but constant t_p, the following two-time correlation functions are accessible:[25–28]

$$F_2^{ss}(t_m,t_p) = \langle \sin[\omega(0)t_p]\sin[\omega(t_m)t_p]\rangle \tag{9}$$

and

$$F_2^{cc}(t_m,t_p) = \langle \cos[\omega(0)t_p]\cos[\omega(t_m)t_p]\rangle. \tag{10}$$

Here, the brackets $\langle\cdots\rangle$ denote ensemble averages. Due to $I=1$, the pulse lengths and phases in ^{6}Li NMR can be adopted from ^{2}H NMR experiments.[25–28] $F_2^{ss}(t_m,t_p)$, the "sin-sin correlation function," results for the pulses 90°_y, 45°_x, and 45°_x in the three pulse sequence, whereas $F_2^{cc}(t_m,t_p)$, the "cos-cos correlation function," is obtained for 90°_y, 90°_y, and 90°_y.

In experimental practice, effects other than ionic jumps result in a decay of the height $I_2^{ss,cc}$ of the ^{6}Li and ^{7}Li stimulated echos. Therefore, we write

$$I_2^{ss,cc}(t_m,t_p) \propto F_2^{ss,cc}(t_m,t_p)F_{SD}(t_m,t_p)\exp\left(-\frac{t_m}{T_1}\right). \tag{11}$$

Here, $F_2^{ss,cc}(t_m,t_p)$ is the loss in correlation due to ionic motion, while $\exp(-t_m/T_1)$ and $F_{SD}(t_m,t_p)$ are the decays due to spin-lattice relaxation and spin diffusion, respectively. The latter is a transport of magnetization due to "flip-flop" processes between dipolar coupled spins. For simplicity, damping due to spin-lattice relaxation is expressed by an exponential function, although it may be somewhat nonexponential. In our samples, $T_1(^6\mathrm{Li}) \gg t_m$, so that it is not necessary to consider this contribution to the stimulated-echo decay. However, the time window is limited by the decay due to spin diffusion $F_{SD}(t_m,t_p)$. Because the effect due to spin diffusion is temperature independent, it can be determined experimentally at low temperatures. By variable temperature experiments, the spin diffusion contribution and the effect of lithium ion dynamics upon the stimulated-echo decay can be conveniently separated (see below). In this way, the rate of ionic hopping motion is available.

Studies on various silver ion conductors have shown that the correlation functions are independent of the value of the evolution time t_p,[32–34] indicating that the NMR frequencies before and after a silver ionic jump are not correlated. Because of the absence of spin diffusion effects in ^{109}Ag, $F_2^{ss} \approx F_2^{cc}$ measures the probability that a silver ion is at the same site in the glass after a time t_m. Specifically,

$$F_2(t_m) \equiv F_2^{cc}(t_m) = F_2^{ss}(t_m) \propto \langle \cos[(\omega_2 - \omega_1)t_p] \rangle, \quad (12)$$

where the term $\cos[(\omega_2-\omega_1)t_p]$ approximates the δ function $\delta(\omega_2-\omega_1)$.[25,28] In general, the evolution time t_p has a similar meaning as the momentum transfer Q in neutron scattering,[61] i.e., it acts as geometrical filter. Since the phase ωt_p enters the two-time correlation functions, small fluctuations in ω are better resolved for large t_p. Thus, the correlation functions for large t_p will decay faster than those for small t_p if the frequencies at neighboring sites are correlated, so that ω will vary step by step. Then, the elementary frequency changes do not result in a significant loss of correlation until t_p is sufficiently large. Due to the much smaller quadrupole moment of ^{6}Li, in relation to ^{7}Li, the evolution times for ^{6}Li should be by a factor of 50 larger than for ^{7}Li.[22]

Because of low signal-to-noise ratios, ^{6}Li correlation functions are difficult to access for samples with natural isotopic abundance (7.4%). To reduce the overall measurement time, we enrich our sample with ^{6}Li nuclei. However, with increasing enrichment, the effects of spin diffusion on the stimulated-echo decay become more pronounced. We varied the ^{6}Li/^{7}Li ratio systematically to find a compromise between sufficient signal-to-noise ratio and acceptable spin diffusion contribution. It turned out that a sample with 50% ^{6}Li enrichment is well suited for stimulated-echo studies of lithium dynamics.

III. EXPERIMENT

The glass $LiPO_3$ was prepared from weighed amounts of Li_2CO_3 and $(NH_4)H_2PO_4$. For the isotopic enrichment, $^6Li_2CO_3$ (ISOTEC, Inc.) containing 95% ^{6}Li was used in appropriate proportion. The starting materials were mixed and preheated at 250 °C for 2 h to remove the reaction byproducts: water and ammonia. The dried mixture was subsequently melted at 800 °C for 30 min. The sample was quenched by pouring the melt onto a copper plate and stored moisture-free. The composition of the glass was checked by ^{31}P magic angle spinning NMR. As typical of the metaphosphate composition, a broad single resonance was observed at about −23 ppm which can be assigned to Q^2 units in the phosphate glass network.[62] The ^{6}Li and ^{7}Li NMR experiments were carried out on a Bruker CXP 300 and a Bruker DSX 400 spectrometer with magnetic field strengths of 7.0 and 9.4 T, respectively. The corresponding Larmor frequencies amount to 44.2 and 58.9 MHz for ^{6}Li and 116.6 and 155.6 MHz for ^{7}Li. A flow of nitrogen gas controlled by a Bruker VT 3000 heating unit was used to adjust the sample temperature. After calibration with $Pb(NO_3)_2$,[63] it is possible to set absolute temperature values within ±2 K. The durations of the 90° rf pulses were 9–12 μs for ^{6}Li and about 3.5 μs for ^{7}Li at the spectrometer with B_0=7.0 T and 4 μs for ^{6}Li at the spectrometer with B_0=9.4 T. Relaxation delays were 20–1000 s for ^{6}Li and 20–60 s for ^{7}Li. The static ^{6}Li NMR spectra were acquired with a solid echo $90^\circ_x - t_p - 90^\circ_y$ with t_p=50 μs. For the static ^{7}Li NMR spectra, a solid echo $90^\circ_x - t_p - 64^\circ_y$ with t_p=30 μs was used.

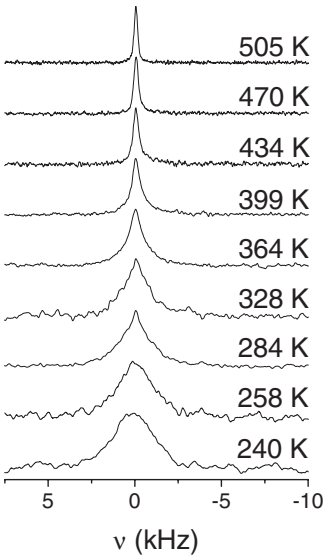

FIG. 1. Temperature-dependent static ^{6}Li NMR spectra of 50% ^{6}Li enriched $LiPO_3$ glass.

IV. RESULTS

A. Line-shape analysis

Figures 1 and 2 show the temperature-dependent ^{6}Li and ^{7}Li NMR spectra of a 50% ^{6}Li enriched $LiPO_3$ glass, respectively. For ^{7}Li, the central Zeeman transition is displayed and analyzed. In both cases, a Lorentzian is observed at high

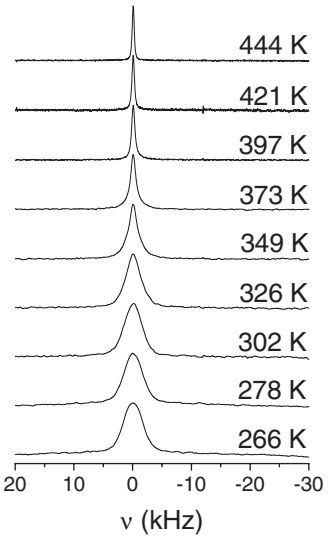

FIG. 2. Temperature-dependent static ^{7}Li NMR spectra of 50% ^{6}Li enriched $LiPO_3$ glass (central line).

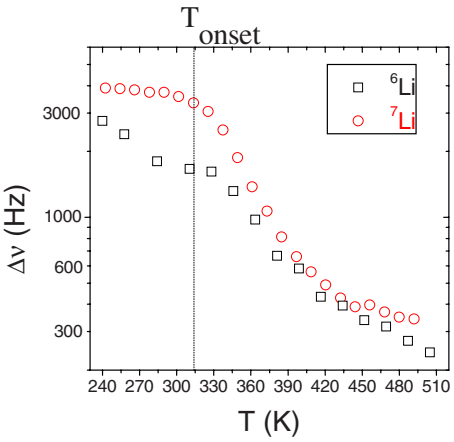

FIG. 3. (Color online) Temperature-dependent full width at half maximum of the static ^{6}Li and ^{7}Li NMR spectra.

temperatures ($T \geqslant 400$ K), while the spectrum at low temperatures ($T \leqslant 300$ K) is approximated by a Gaussian. These findings indicate that, in the former temperature range, fast jumps of all lithium ions lead to an averaging over many different local environments and, hence, resonance frequencies, whereas lithium diffusion is slow on the NMR time scale ($\Delta\omega^{-1} \approx 2$ ms) in the latter temperature range. The temperature-dependent linewidths of the ^{6}Li and ^{7}Li NMR spectra are displayed in Fig. 3. Using Eq. (3), we attempt to roughly estimate the activation energy of the lithium ionic jumps. We obtain a value $E_a = 0.50$ eV, which is substantially smaller than the activation energy from dc conductivity measurements ($E_{dc} = 0.66-0.69$ eV).[13,16] Thus, the formula of Waugh and Fedin underestimates the activation energy of the motional process, consistent with results in the literature.[64] Equation (4) allows us to relate the ^{7}Li linewidths to the correlation times τ_{LS}. Here, we choose the fit parameter $\alpha = 1$ and use $\Delta\nu_0 = 3900$ Hz and $\Delta\nu_\infty = 320$ Hz from the low- and high-temperature limits, respectively. The obtained correlation times show an Arrhenius behavior with $E_a = 0.34$ eV $< E_{dc}$ (see Fig. 4). Thus, application of Eqs. (3) or (4) does not provide access to meaningful activation energies of the lithium ionic jumps in $LiPO_3$ glass, as can be expected for complex molecular dynamics (see Sec. II A).

In ^{109}Ag NMR studies of silver ionic motion in phosphate and borate glasses, it was found that two-phase spectra exist at intermediate temperatures between the limits of slow and

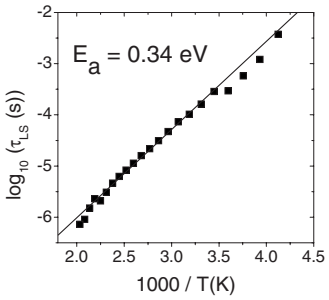

FIG. 4. Temperature-dependent correlation times τ_{LS} calculated by means of Eq. (4) from the ^{7}Li linewidth.

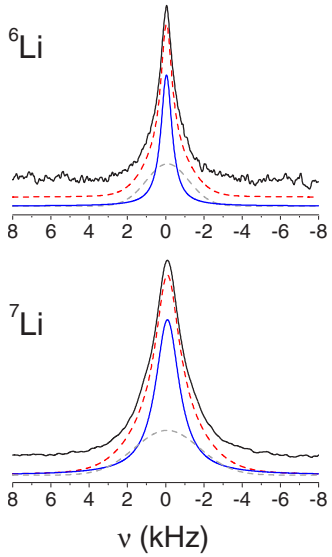

FIG. 5. (Color online) Static ^{6}Li NMR spectra (solid black line) with fit (dashed red line), Gaussian contribution (dashed gray line), and Lorentzian contribution (solid blue line) at 364 K. Static ^{7}Li NMR spectra (solid black line) with fit (dashed red line), Gaussian contribution (dashed gray line), and Lorentzian contribution (solid blue line) at 349 K.

fast motions.[33–35] Closer inspection of Figs. 1 and 2 shows that the ^{6}Li and ^{7}Li NMR line shapes cannot also be described by a single line at temperatures 300 K $\leqslant T \leqslant$ 400 K, but it is necessary to use a superposition of a Gaussian and a Lorentzian (see Fig. 5), where the relative weight of each line-shape component depends on temperature. These two-phase spectra show that, at the same temperature, fast ($\tau \ll \Delta\omega^{-1}$) and slow ($\tau \gg \Delta\omega^{-1}$) lithium ions can be distinguished and a broad distribution of correlation times $G(\log_{10}\tau)$ exists. Due to a larger spectral dispersion, the two-phase nature of previous ^{109}Ag NMR spectra is clearer than that of the present ^{6}Li and ^{7}Li NMR spectra. However, when we fit the ^{6}Li and ^{7}Li NMR spectra with a weighted superposition of a Gaussian and a Lorentzian and keep the position and the width of the Gaussian constrained, as required in the two-phase approach, we obtain good interpolations and stable results. In Fig. 6, the weighting factors $W(T)$ of the Lorentzian line from the integrated amplitudes of the contributions are compared for ^{6}Li and ^{7}Li. As expected, the fraction of the Lorentzian line representing the fast ions decreases as the temperature is lowered.

The temperature dependence of the weighting factor yields information about the shape of the distribution of correlation times $G(\log_{10}\tau)$ (see Sec. II A). The stepless behavior (see Figs. 6–8) shows that $G(\log_{10}\tau)$ is continuous. Assuming that $G(\log_{10}\tau)$ is a logarithmic Gaussian distribution with a temperature-independent width, we can estimate the width parameter σ of the distribution of correlation times based on Eq. (7). Using the linewidths of the low-temperature limit [$\Delta\nu(^6\text{Li}) = 2500$ Hz and $\Delta\nu(^7\text{Li}) = 3900$ Hz] and the activation energy of our ^{6}Li NMR simulated-echo study (see below), we obtain the parameters listed in Table I. The fits resulting from Eq. (7) are included

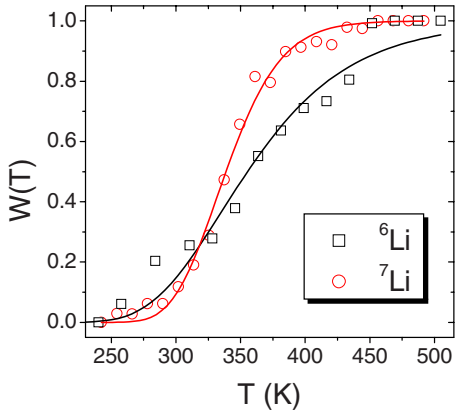

FIG. 6. (Color online) Weighting factors $W(T)$ as obtained by fitting the ^{6}Li and ^{7}Li NMR spectra of a 50% ^{6}Li enriched $LiPO_3$ glass to a superposition of a Gaussian and a Lorentzian. The lines are the fits using Eq. (7).

in Fig. 6. The width parameters amount to 1.65 for ^{6}Li and 0.96 for ^{7}Li corresponding to half widths of 4 (^{6}Li) and 2 (^{7}Li) orders of magnitude, respectively. Thus, the lithium ionic motion is governed by pronounced dynamical heterogeneities. A broader distribution of correlation times is obtained from ^{6}Li NMR data.

On the other hand, assuming that there is a temperature-independent distribution of activation energies, the parameters of this distribution can be obtained from $dW(T)/dT$ according to Eq. (8). The results are shown in Figs. 7 and 8. To remove the scattering of the data, the derivatives were calculated after artificially fitting $W(T)$ to suitable expressions, different from Eq. (7). Since information about τ_0 is not available, we restrict ourselves to show $dW(T)/dT$, which deviates from $g(E_a)$ by a constant factor. The apparent distributions of activation energies differ for ^{6}Li and ^{7}Li, consistent with the result of the above analysis with the first approach. While a broader distribution $g(E_a)$ is obtained

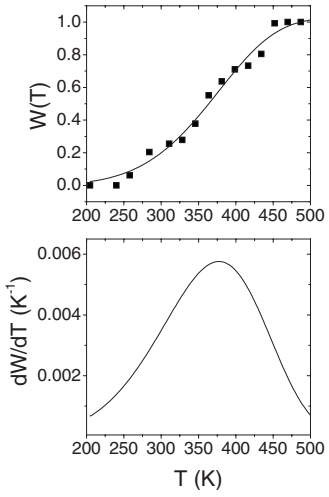

FIG. 7. Upper panel: Temperature dependence of the fraction $W(T)$ of the fast ^{6}Li ions; the line is a fit with a suitable function. Lower panel: Corresponding derivative dW/dT.

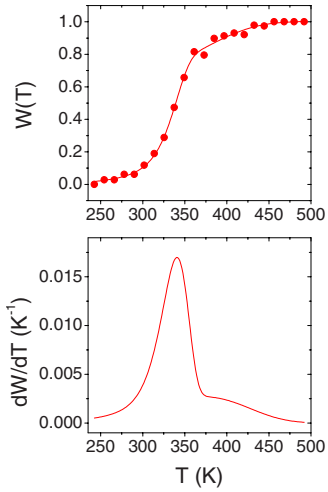

FIG. 8. (Color online) Upper panel: Temperature dependence of the fraction $W(T)$ of the fast ^{7}Li ions; the line is a fit with a suitable function. Lower panel: Corresponding derivative dW/dT.

from the analysis of the ^{6}Li NMR data, a more asymmetric shape is obtained from the ^{7}Li NMR data. Since the lithium ionic motion should be very similar for both nuclei, hardly any difference is expected at first glance. However, it is necessary to consider that the contributions of dipolar and quadrupolar couplings to the ^{6}Li and ^{7}Li NMR spectra differ. For ^{7}Li, there is only the dipolar contribution and, hence, the linewidth reflects a multiparticle correlation function, i.e., not only the motion of a given nucleus, but also that of the neighboring ^{7}Li ions leads to line narrowing. In contrast, both quadrupolar and dipolar couplings contribute to ^{6}Li NMR spectra so that the change in linewidth corresponds to a superposition of a single particle and a multiparticle correlation function. These differences result in diverse line narrowing behaviors, as observed via ^{6}Li and ^{7}Li NMRs. In the literature, similar arguments were used to explain differences of ^{6}Li and ^{7}Li spin-lattice relaxation behaviors relating to ion dynamics.[5]

B. Two-time correlation functions

Next, we demonstrate that ^{6}Li NMR stimulated-echo spectroscopy provides straightforward access to the two-time correlation function of the lithium ionic hopping motion in $LiPO_3$ glass. In Fig. 9, the ^{6}Li stimulated-echo decays $I_2^{ss}(t_m;t_p=100\ \mu s)$ are presented. Lithium ionic jumps lead to temperature-dependent, nonexponential decays of $I_2^{ss}(t_m)$. As the lithium ionic motion slows down with decreasing temperature, the decays are shifted successively toward longer

TABLE I. Parameters characterizing the distribution of correlation times using Eq. (7).

	σ	τ_0 (s)
^{6}Li	1.65 ± 0.16	$1.74 \times 10^{-13} \pm 4.38 \times 10^{-14}$
^{7}Li	0.96 ± 0.05	$3.88 \times 10^{-14} \pm 3.11 \times 10^{-15}$

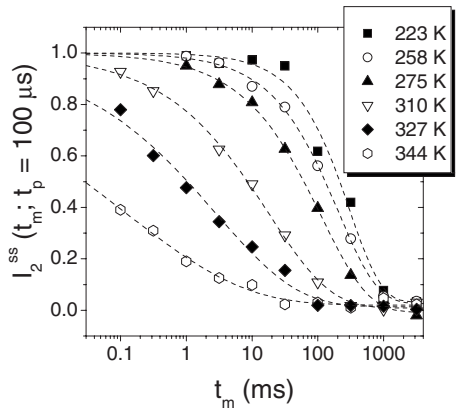

FIG. 9. ^{6}Li NMR stimulated-echo decays $I_2^{ss}(t_m;t_p=100\ \mu s)$ of $LiPO_3$ glass at various temperatures. Dashed lines: Interpolations with a KWW function.

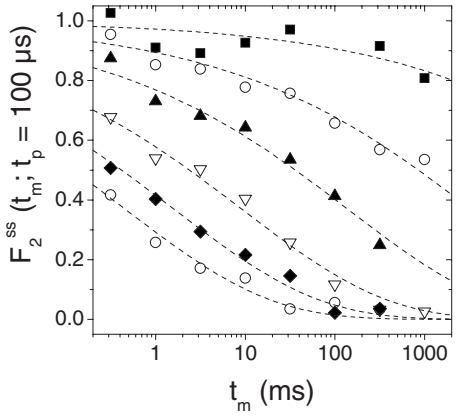

FIG. 11. ^{6}Li NMR two-time correlation functions $F_2^{ss}(t_m;t_p=100\ \mu s)$ of $LiPO_3$ glass at various temperatures after spin diffusion correction. The symbols represent the same temperatures as in Fig. 9. Dashed lines: Interpolations with a KWW function.

mixing times. Since the spin-lattice relaxation time T_1 is of the order of 60 s at the highest temperature studied and even longer at lower temperatures, the ^{6}Li two-time correlation functions are not damped by relaxation effects. However, when the temperature is decreased, the correlation functions become more exponential and the shift of the curves ceases at low temperatures. These findings indicate that ion dynamics do no longer dominate the stimulated-echo decay at low temperatures. Rather, the decays are governed by the temperature-independent effect of spin diffusion. This behavior contrasts previous results from ^{109}Ag NMR studies on silver ion conductors.[32–34,36] In the latter case, spin diffusion is very slow, owing to the small magnetic moments of the silver nuclei, so that the stimulated-echo decay is not influenced by this effect, leading to a temperature-independent nonexponentiality of the correlation functions.

We analyze the stimulated-echo decay in Fig. 9 by fitting the data to a KWW function. Actually, the experimental data are scaled to yield an amplitude of 1 in these interpolations. The fit parameters, τ and β, are displayed in Fig. 10. The parameter β is a measure of the nonexponentiality of the decays. It increases toward the limiting value of $\beta=1$ upon cooling, showing that more and more of the decay due to the ionic jump motion is cut off by the more exponential decay due to spin diffusion. Likewise, the temperature-independent effect of spin diffusion leads to an apparent plateau for τ at

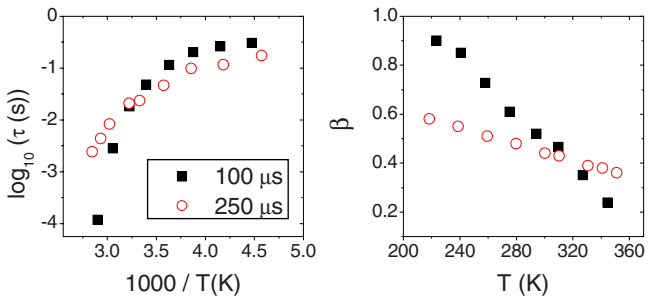

FIG. 10. (Color online) τ and β as extracted from KWW fits to the stimulated-echo decays $I_2^{ss}(t_m;t_p)$ of $LiPO_3$ glass for different evolution times.

low temperatures. Determining the spin diffusion contribution from the low-temperature data, their effect upon the higher-temperature data can be removed. We obtain experimentally a spin diffusion factor of $F_{SD}(t_m;t_p=100\ \mu s)=\exp[-(t_m/370\ \text{ms})^{0.9}]$. Multiplying the data with the inverse of the spin diffusion factor, two-time correlation functions are accessible, the decays of which are solely due to lithium ionic jumps. These correlation functions are shown in Fig. 11. Strongly nonexponential decays are observed, which continuously shift to longer mixing times when the temperature is lowered.

The corrected correlation functions are also fitted to a KWW function. Consistent with results from ^{109}Ag NMR correlation functions of silver phosphate glasses,[33,34] we find no evidence for a systematic temperature dependence of β. Therefore, we fix the stretching parameter at the mean of the observed values, $\beta=0.27$, yielding stable fits and good interpolations (see Fig. 11). Thus, stretching parameters of $\beta=0.27\pm0.03$ characterize the correlation functions at all temperatures, indicating that the lithium ionic hopping motion in $LiPO_3$ glass is a strongly nonexponential dynamical process. Based on the fit parameters, the mean correlation time $\langle\tau_{2t}\rangle$ can be calculated according to $\langle\tau_{2t}\rangle=(\tau/\beta)\Gamma(1/\beta)$, where Γ denotes the gamma function. The results are displayed in Fig. 12. When fitting the data to an Arrhenius law, an activation energy $E_a=0.66$ eV is found. This value is in excellent agreement with the activation energies determined with other techniques ($E_a=0.6-0.7$ eV).[13,16,17,20]

In Fig. 12, we also compare the mean correlation times $\langle\tau_{2t}\rangle$ from the present stimulated-echo experiments with that reported in previous mechanical and electrical relaxation studies on $LiPO_3$ glass, where the relation $\tau_\sigma=\frac{\epsilon_0\epsilon_\infty}{\sigma_{dc}}$ was employed to obtain time constants from the electric conductivities.[16] We see that the mean correlation times resulting from the different experimental techniques agree well. By contrast, the time constants τ_{LS} obtained from the ^{7}Li linewidths differ substantially from the other data, clearly demonstrating that NMR line-shape analysis does not pro-

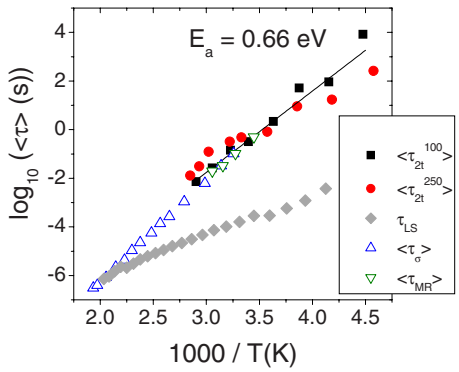

FIG. 12. (Color online) Comparison of mean correlation times of the lithium dynamics in $LiPO_3$ glass from different experimental techniques. The correlation times $\langle\tau_{2t}^{100}\rangle$ and $\langle\tau_{2t}^{250}\rangle$ are extracted from KWW fits to the sin-sin correlation functions $F_2^{ss}(t_m;t_p)$ for t_p=100 μs and t_p=250 μs, respectively, after spin diffusion correction. The time constants τ_{LS} were obtained from the ^{7}Li NMR line shape according to Eq. (4) (see Fig. 4). The correlation times τ_σ and τ_{MR} are from dc conductivity and mechanical relaxation experiments, respectively (Ref. 16).

vide reliable correlation times and activation energies in studies of ion dynamics in glasses.

Figure 10 also shows the parameters from KWW fits to I_2^{ss} for an evolution time t_p=250 μs. Evidently, β exhibits a weaker apparent temperature dependence for the larger evolution time. From the fit, we obtain a spin diffusion factor of $F_{SD}(t_m;t_p=250\ \mu\text{s})=\exp[(-t_m/250\ \text{ms})^{0.61}]$. Again, we multiply the experimental data with the inverse of this factor to extract the decay due to ionic motion. Fitting these corrected data for t_p=250 μs to a KWW function, we obtain a mean value of β=0.33 and the mean correlation times $\langle\tau_{2t}\rangle$ included in Fig. 12. While for higher temperatures $\langle\tau_{2t}\rangle$ hardly depends on the evolution time, the effect of spin diffusion cannot be removed completely from the two-time correlation functions at low temperatures. We conclude that the evolution time should be set as small as possible when investigating lithium ion dynamics by means of two-time correlation spectroscopy.[31]

V. DISCUSSION AND SUMMARY

In the present contribution, we have characterized the lithium ion dynamics of glassy $LiPO_3$ using ^{6}Li und ^{7}Li NMR techniques. Line-shape analysis of temperature-dependent ^{6}Li and ^{7}Li NMR spectra has provided information about lithium ionic jumps on the time scale of microsecond to millisecond. The apparent activation energies found by two traditional data analysis methods are substantially smaller than the value obtained by other experimental techniques. Such deviations have been observed in several NMR line-shape studies of ionic motion in solid electrolytes.[57,64–66] Most likely, they are due to the fact that the line-shape analysis methods rely on the inherent assumption of an exponentially decaying correlation function, while the ionic jumps are characterized by strongly nonexponential correlation functions. We conclude that NMR line-shape analysis does not yield reliable correlation times of ion dynamics in glasses.

By contrast, ^{6}Li NMR stimulated-echo spectroscopy provides quantitative microscopic insights into ionic jumps in the millisecond to second regime. In general, both ion dynamics and spin diffusion contribute to the ^{6}Li stimulated-echo decays. However, their effects can be successfully separated by virtue of temperature-dependent measurements. For optimum separation, the evolution time should be set as small as possible. The two-time correlation functions, which remain after removal of the spin diffusion contribution, reflect the single ionic jump dynamics. Specifically, they provide access to the probability of finding a lithium ion at the same site at a later time. For $LiPO_3$ glass, the mean correlation times $\langle\tau_{2t}\rangle$ resulting from the present ^{6}Li NMR two-time correlation functions agree well with that obtained from electrical and mechanical relaxation measurements.[17] Likewise, the activation energy E_a=0.66 eV from ^{6}Li NMR two-time correlation spectroscopy agrees with results from other techniques, e.g., E_{dc}=0.66 eV.[13,17] This demonstrates that unlike other NMR techniques, stimulated-echo spectroscopy enables a quantitative study of the elementary steps of the long-range charge transport, consistent with conclusions of a ^{7}Li stimulated-echo study on a crystalline ion conductor.[67]

The correlation functions of the lithium ionic jumps are well described by a KWW function with a small stretching parameter $\beta=0.27\pm0.03$, indicating a pronounced nonexponential relaxation. In the past, several models were set forward to explain the origin of this strong nonexponentiality, which is a key feature of ion dynamics in solids.[6–12] The ^{6}Li und ^{7}Li NMR line shapes have shed some light on this issue for $LiPO_3$ glass. A closer inspection of the spectra has revealed a two-phase behavior at suitable temperatures, indicating the coexistence of fast and slow ions, i.e., the presence of a broad distribution of correlation times. Of course, this finding does not exclude other contributions to the nonexponential ionic relaxation. For higher temperatures, MD simulations on glassy ion conductors revealed that, in addition to dynamical heterogeneities, forward-backward jumps add to the nonexponentiality.[20,21,68–71]

To gain further insights into the relevance of dynamical heterogeneities, we have estimated the width of the distribution of correlation times $G(\log_{10}\tau)$ based on the temperature-dependent ^{6}Li line shapes, yielding a width of about 4 orders of magnitude in the studied temperature range. The question arises whether a distribution of this width is sufficient to explain the pronounced nonexponentiality of the two-time correlation functions. Assuming that the latter is exclusively due to the existence of such distribution, the stretching parameter is related to the logarithmic width Δ of $G(\log_{10}\tau)$ according to $\beta\approx0.93/\left(\frac{\Delta}{1.14}-0.06\right)$.[72] Then, $\Delta\approx4$ translates into $\beta\approx0.27$, nicely consistent with the observed nonexponentiality of the correlation functions. This agreement suggests that the existence of a broad distribution of correlation times is indeed a major contribution to the nonexponential ionic relaxation in $LiPO_3$ glass. A substantially smaller distribution of correlation times has been inferred from the temperature-dependent ^{7}Li NMR spectra, specifically, from the linewidth of the central line. We be-

lieve that this discrepancy reflects the fact that the contributions from single particle and from multiparticle effects to the line shapes are significantly different for ^{6}Li and ^{7}Li nuclei, as was argued in the literature.[5]

The results of the present study on the lithium dynamics in $LiPO_3$ glass are in conceptual agreement with findings of previous ^{109}Ag NMR studies on the silver ionic motion in phosphate and borate glasses.[32–36] Specifically, it was found that nonexponential correlation functions with small stretching parameters $\beta \approx 0.2$ characterize the silver ionic jumps in these glasses. Moreover, the observation of ^{109}Ag NMR two-phase spectra demonstrated the existence of a distribution of correlation times. For the silver ionic motion, ^{109}Ag NMR three-time correlation functions enabled a quantitative investigation of the origin of the nonexponential relaxation. The analysis indicated for a number of crystalline and glassy silver ion conductors that, in large parts, the nonexponentiality is due to the existence of dynamical heterogeneities, rather than to intrinsically nonexponential relaxation.[33,35,36,38] More quantitative insights on this issue in $LiPO_3$ glass will be discussed on the basis of ^{6}Li NMR three-time correlation functions in a future publication.

ACKNOWLEDGMENTS

This work was supported by the Deutsche Forschungsgemeinschaft within the SFB 458 programme. S.F. thanks the Fonds der Chemischen Industrie.

*mivogel@uni-muenster.de

[1] J. T. S. Irvine and A. R. West, in *High Conductivity Solid Ionic Conductors*, edited by T. Takahashi (World Scientific, Singapore, 1989).
[2] G. Y. Adachi, N. Imanaka, and H. Aono, Adv. Mater. (Weinheim, Ger.) **8**, 127 (1996).
[3] M. Duclot and J.-L. Souquet, J. Power Sources **97-98**, 610 (2001).
[4] T. Minami, A. Hayashi, and M. Tatsumisago, Solid State Ionics **177**, 2715 (2006).
[5] K. L. Ngai, J. Non-Cryst. Solids **203**, 232 (1996).
[6] M. D. Ingram, Philos. Mag. B **60**, 729 (1989).
[7] K. L. Ngai, S. L. Peng, and K. Y. Tsang, Physica A **191**, 523 (1992).
[8] K. Funke, Prog. Solid State Chem. **22**, 111 (1995).
[9] S. R. Elliott, Solid State Ionics **70-71**, 27 (1994).
[10] A. Bunde, M. D. Ingram, and P. Maass, J. Non-Cryst. Solids **172-174**, 1222 (1994).
[11] H. Kahnt, J. Non-Cryst. Solids **203**, 225 (1996).
[12] S. D. Baranovskii and H. Cordes, J. Chem. Phys. **111**, 7546 (1999).
[13] D. L. Sidebottom, P. F. Green, and R. K. Brow, J. Non-Cryst. Solids **183**, 151 (1995).
[14] E. Göbel, W. Müller-Warmuth, H. Olyschläger, and H. Dutz, J. Magn. Reson. (1969-1992) **36**, 371 (1979).
[15] P. F. Green, D. L. Sidebottom, and R. K. Brow, J. Non-Cryst. Solids **172-174**, 1353 (1994).
[16] P. F. Green, D. L. Sidebottom, R. K. Brow, and J. J. Hudgens, J. Non-Cryst. Solids **231**, 89 (1998).
[17] P. F. Green, E. F. Brown, and R. K. Brow, J. Non-Cryst. Solids **255**, 87 (1999).
[18] R. Kohlrausch, Ann. Phys. **91**, 179 (1854).
[19] G. Williams and D. C. Watts, Trans. Faraday Soc. **66**, 80 (1970).
[20] M. Vogel, Phys. Rev. B **68**, 184301 (2003).
[21] M. Vogel, Phys. Rev. B **70**, 094302 (2004).
[22] R. Böhmer, K. R. Jeffrey, and M. Vogel, Prog. Nucl. Magn. Reson. Spectrosc. **47**, 87 (2007), and references therein.
[23] E. Rössler, M. Taupitz, K. Börner, M. Schulz, and H.-M. Vieth, J. Chem. Phys. **92**, 5847 (1990).
[24] M. Vogel and T. Torbrügge, J. Chem. Phys. **125**, 054905 (2006).
[25] K. Schmidt-Rohr and H. W. Spiess, *Multidimensional Solid-State NMR and Polymers* (Academic, London, 1994).
[26] R. Böhmer and F. Kremer, *Broadband Dielectric Spectroscopy* (Springer-Verlag, Berlin, 2002).
[27] E. A. de Azevedo, T. J. Bonagamba, and D. Reichert, Prog. Nucl. Magn. Reson. Spectrosc. **47**, 137 (2005).
[28] R. Böhmer, G. Diezemann, G. Hinze, and E. Rössler, Prog. Nucl. Magn. Reson. Spectrosc. **39**, 191 (2001).
[29] R. Böhmer, T. Jörg, F. Qi, and A. Titze, Chem. Phys. Lett. **316**, 419 (2000).
[30] V. W. J. Verhoeven, I. M. de Schepper, G. Nachtegaal, A. P. M. Kentgens, E. M. Kelder, J. Schoonman, and F. M. Mulder, Phys. Rev. Lett. **86**, 4314 (2001).
[31] F. Qi, T. Jörg, and R. Böhmer, Solid State Nucl. Magn. Reson. **22**, 484 (2002).
[32] M. Vogel, C. Brinkmann, H. Eckert, and A. Heuer, J. Non-Cryst. Solids **307-310**, 971 (2002).
[33] M. Vogel, C. Brinkmann, H. Eckert, and A. Heuer, Phys. Chem. Chem. Phys. **4**, 3237 (2002).
[34] M. Vogel, C. Brinkmann, H. Eckert, and A. Heuer, Solid State Nucl. Magn. Reson. **22**, 344 (2002).
[35] S. Berndt, K. R. Jeffrey, R. Küchler, and R. Böhmer, Solid State Nucl. Magn. Reson. **27**, 122 (2005).
[36] M. Vogel, C. Brinkmann, H. Eckert, and A. Heuer, Phys. Rev. B **69**, 094302 (2004).
[37] F. Qi, C. Rier, R. Böhmer, W. Franke, and P. Heitjans, Phys. Rev. B **72**, 104301 (2005).
[38] C. Brinkmann, S. Faske, M. Vogel, T. Nilges, A. Heuer, and H. Eckert, Phys. Chem. Chem. Phys. **8**, 369 (2006).
[39] M. Vogel, C. Brinkmann, H. Eckert, and A. Heuer, J. Non-Cryst. Solids **352**, 5156 (2006).
[40] M. Wilkening, W. Küchler, and P. Heitjans, Phys. Rev. Lett. **97**, 065901 (2006).
[41] M. Wilkening and P. Heitjans, Solid State Ionics **177**, 3031 (2006).
[42] M. Vogel and T. Torbrügge, J. Chem. Phys. **125**, 164910 (2006).
[43] L. van Wüllen, T. Echelmeyer, H.-W. Meyer, and D. Wilmer, Phys. Chem. Chem. Phys. **9**, 3298 (2007).
[44] Z. Xu and J. F. Stebbins, Science **270**, 1332 (1995).
[45] J. L. Bjorkstam, J. Listerud, and M. Villa, Magn. Reson. Rev. **6**, 1 (1980).
[46] O. Kanert, Phys. Rep. **91**, 182 (1982).

[47] P. A. Beckmann, Phys. Rep. **171**, 85 (1988).
[48] J. F. Stebbins, Chem. Rev. (Washington, D.C.) **91**, 1353 (1991).
[49] D. Brinkmann, Prog. Nucl. Magn. Reson. Spectrosc. **24**, 527 (1992).
[50] P. Heitjans and S. Indris, J. Phys.: Condens. Matter **15**, R1257 (2003).
[51] P. Heitjans, S. Indris, and M. Wilkening, Diffusion Fundamentals **2**, 45 (2005).
[52] M. Trunnell, D. R. Torgeson, S. W. Martin, and F. Borsa, J. Non-Cryst. Solids **139**, 257 (1992).
[53] R. Böhmer, J. Magn. Reson. **147**, 78 (2000).
[54] M. Wilkening, D. Gebauer, and P. Heitjans, J. Phys.: Condens. Matter **20**, 22201 (2008).
[55] J. S. Waugh and E. I. Fedin, Solid State Phys. **4**, 2233 (1962).
[56] N. Bloembergen, E. M. Purcell, and R. V. Pound, Phys. Rev. **73**, 679 (1948).
[57] M. Wilkening, D. Bork, S. Indris, and P. Heitjans, Phys. Chem. Chem. Phys. **4**, 3246 (2002).
[58] B. Roling, C. Martiny, and S. Brückner, Phys. Rev. B **63**, 214203 (2001).
[59] S. Summerfield, Philos. Mag. B **52**, 9 (1985).
[60] S. J. Pas, R. D. Banhatti, and K. Funke, Solid State Ionics **177**, 3135 (2006).
[61] F. Fujara, S. Wefing, and W. F. Kuhs, J. Chem. Phys. **88**, 6801 (1988).
[62] L. van Wüllen, H. Eckert, and G. Schwering, Chem. Mater. **12**, 1840 (2000).
[63] P. A. Beckmann and C. Dybowski, J. Magn. Reson. **146**, 379 (2000).
[64] M. Grüne, W. Müller-Warmuth, P. zum Hebel, and B. Krebs, Solid State Ionics **66**, 165 (1993).
[65] S. G. Bishop and P. J. Bray, J. Chem. Phys. **48**, 1709 (1968).
[66] T. Matsuo, M. Shibasaki, and T. Katsumata, Solid State Ionics **154-155**, 759 (2002).
[67] M. Wilkening, C. Mühle, M. Jansen, and P. Heitjans, J. Phys. Chem. B **111**, 8691 (2007).
[68] J. Habasaki and Y. Hiwatari, Phys. Rev. E **65**, 021604 (2002).
[69] E. Sunyer, P. Jund, and R. Jullien, Phys. Rev. B **65**, 214203 (2002).
[70] A. Heuer, M. Kunow, M. Vogel, and R. D. Banhatti, Phys. Rev. B **66**, 224201 (2002).
[71] H. Lammert, M. Kunow, and A. Heuer, Phys. Rev. Lett. **90**, 215901 (2003).
[72] R. Böhmer, J. Non-Cryst. Solids **172-174**, 628 (1994).